

Disorder Dependence of Interface Spin Memory Loss

Kriti Gupta,¹ Rien J.H. Wesselink,¹ Ruixi Liu,² Zhe Yuan,^{2,*} and Paul J. Kelly^{1,2,†}

¹*Faculty of Science and Technology and MESA⁺ Institute for Nanotechnology, University of Twente, P.O. Box 217, 7500 AE Enschede, The Netherlands*

²*The Center for Advanced Quantum Studies and Department of Physics, Beijing Normal University, 100875 Beijing, China*

(Dated: February 3, 2020)

The discontinuity of a spin-current through an interface caused by spin-orbit coupling is characterized by the spin memory loss (SML) parameter δ . We use first-principles scattering theory and a recently developed local current scheme to study the SML for Au|Pt, Au|Pd, Py|Pt and Co|Pt interfaces. We find a minimal temperature dependence for nonmagnetic interfaces and a strong dependence for interfaces involving ferromagnets that we attribute to the spin disorder. The SML is larger for Co|Pt than for Py|Pt because the interface is more abrupt. Lattice mismatch and interface alloying strongly enhance the SML that is larger for a Au|Pt than for a Au|Pd interface. The effect of the proximity induced magnetization of Pt is negligible.

With the discovery of the giant magnetoresistance (GMR) effect in magnetic multilayers,^{1,2} it was recognized that interfaces play a key role in spin transport phenomena. In semiclassical formulations³⁻⁵ of transport, these appear as discrete resistances and the description of the transport of electrons through a multilayer requires a resistivity ρ for each material as well as a resistance R_{Γ} for each interface. Bulk resistivities are readily measured, interface resistances much less so. Magnetic materials require spin-dependent bulk resistivities ρ_{σ} and interface resistances R_{σ} . Because spin is not conserved, describing its transport additionally requires a spin-flip diffusion length (SDL) l_{sf} in each material, as well as its counterpart for each interface, the spin memory loss (SML) parameter δ . Determining l_{sf} requires distinguishing interface and bulk contributions. Because doing so is non-trivial, the interface contribution had been largely neglected and values of l_{sf} reported over the last decade for well studied materials like Pt span an order of magnitude.⁶⁻⁸

Almost everything we know about interface parameters is from current-perpendicular-to-the-plane (CPP) magnetoresistance experiments^{5,6,9} interpreted using the semiclassical Valet-Fert (VF) model.⁴ Though these experiments are relatively simple to interpret, they are restricted to low temperatures as they require superconducting leads⁵ while calculations have so far only addressed ballistic interfaces.¹⁰⁻¹⁵ Because the vast majority of experimental studies in spintronics is carried out at room temperature, there is a need to know how transport parameters, in particular those describing interfaces, behave at finite temperatures.

This need is accentuated by the huge interest in recent years^{7,16} in the spin Hall effect (SHE)¹⁷⁻¹⁹ whereby a longitudinal charge current drives a transverse spin current in nonmagnetic materials, and in its inverse, the inverse SHE (ISHE). Determination of the spin Hall angle (SHA) Θ_{sH} that measures the efficiency of the SHE is intimately connected with the SDL and, because an interface is always involved, with the SML.²⁰ When use is made of spin pumping and the ISHE²¹⁻²⁴ or the SHE and

spin-transfer torque (STT),²⁵ the interface in question is between ferromagnetic (FM) and nonmagnetic (NM) materials. When the nonlocal spin-injection method is used,^{26,27} two interfaces are involved: an FM|NM interface to create a spin accumulation and an NM|NM' interface to detect it. Progress has been made by recognizing that bulk parameters like l_{sf} and Θ_{sH} are very sample dependent and that the SML plays a key role in determining their values.^{20,28-30} Recent studies suggesting that measurements of the SHA may actually be dominated by interface effects^{20,28,31,32} are stimulating attempts to tailor these.³³⁻³⁷

This makes it crucial to have a way to independently determine interface parameters. We recently described a formalism to evaluate local charge and spin currents⁸ from the solutions of fully relativistic quantum mechanical scattering calculations³⁸ that include temperature-induced lattice and spin disorder.^{39,40} This yielded a layer-resolved description of spin currents propagating through atomic layers of thermally disordered Pt and Py that allowed us to unambiguously determine bulk transport properties.⁴¹ By focussing on spin currents, we can straightforwardly evaluate all the parameters entering the Valet-Fert semiclassical formalism⁴ that is universally used to interpret experiment.⁵

In this paper we focus on interface transport properties and study realistic interfaces between thermally disordered materials. Typical structures used in experimental studies of the SHE contain a heavy NM metal with strong SOC and a 3d transition metal (TM) or TM alloy ferromagnet.^{7,20-25,44} We will study (i) Au|Pt and Au|Pd interfaces to shed light on the role of SOC and roughness at interfaces involving heavy TMs and (ii) Py|Pt and Co|Pt interfaces to examine the role of the FM magnetization and disorder in determining interface parameters, as well as the temperature dependence of all these.

Method.—We begin by solving the VF equations analytically for the spin accumulation $\mu_{si}(z)$ and spin current $j_{si}(z)$ in a metallic multilayer. The solution in each region i involves two coefficients A_i and B_i that are determined by appropriate boundary conditions.⁴ For an

NM|NM' system we will require that $j_s(0) = 1$ at the left-lead|NM interface corresponding to injecting a fully spin polarized current from the left lead and that $j_s(\infty) = 0$ requiring the NM' material to be much thicker than its l_{sf} value. The interface (I) is initially considered as a bulklike material with resistivity ρ_I , SDL $l_I \equiv l_{sf}^I$ and thickness t so that at the NM|I and I|NM' interfaces the spin accumulation and spin current are continuous.^{45,46} We then eliminate the coefficients A_I and B_I and take the limit $t \rightarrow 0$ thereby defining the areal interface resistance AR_I and the SML parameter δ as

$$AR_I = \lim_{t \rightarrow 0} \rho_I t \quad \text{and} \quad \delta = \lim_{t \rightarrow 0} t/l_I. \quad (1)$$

We finally express δ as

$$\frac{j_{s,NM}(z_I)}{j_{s,NM'}(z_I)} = \cosh \delta + \frac{\rho_{NM'} l_{NM'}}{AR_I} \delta \sinh \delta \quad (2)$$

in terms of $j_{si}(z_I)$, the spin current at the interface z_I on the $i = \text{NM}$ and NM' sides as well as $\rho_{NM'}$, $l_{NM'} \equiv l_{sf}^{NM'}$ and R_I . The relationship of the SML to the spin current discontinuity $j_{s,NM}(z_I) - j_{s,NM'}(z_I)$ is nontrivial.

Au|Pt interface.—We illustrate our methodology in Fig. 1 for a Au|Pt interface between “room-temperature” (RT) Au and Pt in which a Gaussian distribution of atomic displacements in a 7×7 lateral supercell was used to reproduce the experimentally observed resistivities of each bulk material at $T=300\text{K}$, $\rho_{\text{Au}} = 2.3\mu\Omega\text{cm}$ and $\rho_{\text{Pt}} = 10.7\mu\Omega\text{cm}$ ⁴⁷ for which $l_{\text{Au}} \sim 80\text{nm}$ and $l_{\text{Pt}} \sim 5.25 \pm 0.05\text{nm}$.⁸ The empty grey circles in Fig. 1 represent $j_s(z)$ obtained⁴⁸ from the results of quantum mechanical scattering calculations³⁸ for a Au|Pt bilayer when a fully polarized spin current was injected into the bilayer from the left Au lead. The lattice constant of fcc Au is initially chosen to be that of Pt ($a'_{\text{Au}} = a_{\text{Pt}} = 3.923\text{\AA}$) which does not affect the Au electronic structure qualitatively. The figure also shows the VF solutions in Au (blue curve) and Pt (red curve) found by fitting $j_s(z)$ far from the interface. The initial spatial decay of $j_s(z)$ is determined by l_{Au} , the rapid decay in the vicinity of the interface is described in the semiclassical VF framework by the interface discontinuity and, after this abrupt decay, the spin current that survives in Pt decays to zero on a length scale described by l_{Pt} .

By fitting $j_s(z)$ to the solution of the VF equation, we obtain values of $j_{s,\text{Au}}(z_I)$ and $j_{s,\text{Pt}}(z_I)$. From the Landauer expression for the conductance in terms of the transmission matrices, $AR_I = 0.54 \pm 0.03\text{f}\Omega\text{m}^2$ is directly determined leaving just δ as the only unknown parameter. Using a numerical root finder to solve (2), we find $\delta = 0.62 \pm 0.03$ where the error bar is evaluated from the uncertainties in the other parameters.

The bulk parameters ρ_{Pt} and $1/l_{\text{Pt}}$ are known to increase linearly with temperature^{31,40,47,49} but virtually nothing is known about the temperature dependence of interface parameters. We therefore calculate $AR_{\text{Au|Pt}}$ and δ at 200 and 400 K and plot the results in Fig. 1 (inset). Within the error bars of the calculations, both

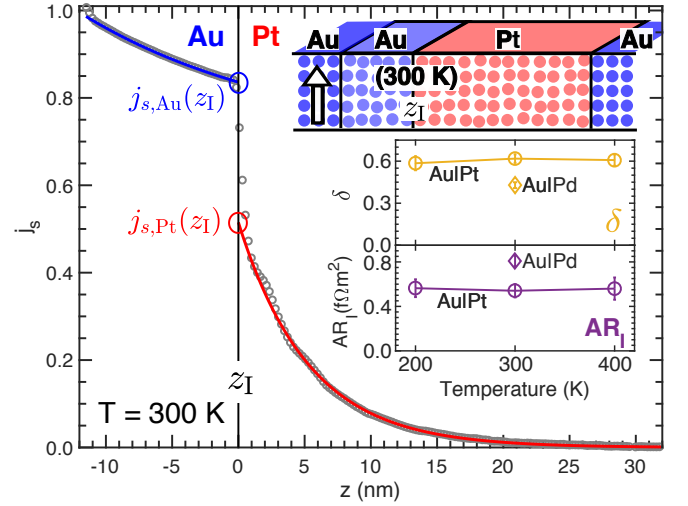


FIG. 1. A fully polarized spin-current j_s injected at 300 K from the left Au lead into a Au(50)|Pt(140) bilayer sandwiched between Au leads decays exponentially in Au and in Pt; the numbers in brackets denote the number of atomic layers. The solid lines indicate fits for $j_s(z)$ in individual layers using solutions of the VF equations. Inset (top panel): schematic of the scattering region. (Middle and bottom panels): temperature dependence of the interface parameters δ (yellow) and R_I (purple) for a Au|Pt interface (circles). The corresponding parameters for Au|Pd at 300 K are included (diamonds).

parameters remain constant between 200 and 400 K. The temperature independence that we observe for δ is in agreement with the results of a very recent CPP-MR experimental study for Cu|Pt interface that shows δ to be nearly constant over the temperature range 0-300 K.⁵⁰

Interface Mixing.—Unlike the sharp interfaces between bulk Au and Pt we have considered so far, experimental interfaces are believed to comprise a few intermixed layers. To study the effect of interface mixing, we insert N atomic layers of $\text{Au}_{50}\text{Pt}_{50}$ random alloy at the interface of the lattice-matched Au|Pt bilayer.⁵¹ The results for the spin current $j_s(z)$ and corresponding values of δ at 300 K are shown in Fig. 2 for $N = 0, 2, 4$. When the spin current from bulk Au approaches the mixed interface layers (yellow for $N = 2$, green for $N = 4$), then compared to the sharp interface, $j_s(z)$ decreases more and δ increases rapidly with increasing N (inset). Electron scattering at a commensurate and clean Au|Pt interface only involves Bloch states with equal \mathbf{k}_{\parallel} but intermixing (and thermal disorder) break momentum conservation and allow $\mathbf{k}_{\parallel} \rightarrow \mathbf{k}'_{\parallel}$ scattering. The higher scattering rate results in a higher spin-flipping probability and hence a larger δ for the intermixed interfaces. Moreover, conduction electrons injected into Au are only weakly affected by SOC until they enter Pt where as d states they become very susceptible to the large SOC. The interatomic mixing effectively increases the region where conduction electrons experience large SOC and therefore increases the SML.

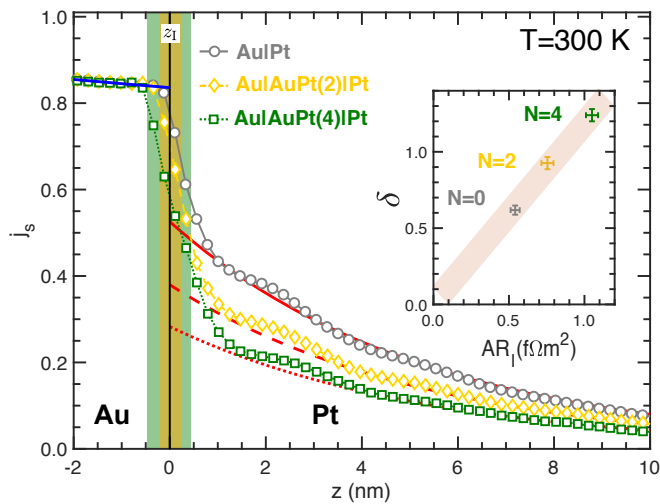


FIG. 2. A fully polarized spin current $j_s(z)$ is injected into a Au|Pt bilayer with: a sharp interface (vertical black line), 2 layers of Au₅₀Pt₅₀ interface (yellow shaded region) and 4 layers of Au₅₀Pt₅₀ interface (green shaded region) between them. The calculated spin currents $j_s(z)$ for the three cases are shown as gray circles, yellow diamonds and green squares respectively. The solid blue line indicates a fit to the VF equation in Au. The solid, dashed and dotted red lines indicate fits to the VF equation in Pt for Au|Pt, Au|Au₅₀Pt₅₀(2)|Pt and Au|Au₅₀Pt₅₀(4)|Pt respectively. (Inset) δ vs AR_I for $N = 0, 2$ and 4 interface layers of mixed Au₅₀Pt₅₀.

The interface resistance AR_I also increases monotonically as the disordered region increases in thickness suggesting that $\delta \propto AR_I$ so $\rho_l l_I \sim \text{const}$.

Lattice Mismatch.—To study the effect of $\mathbf{k}_{\parallel} \rightarrow \mathbf{k}'_{\parallel}$ scattering on its own, we re-examine the sharp (111) Au|Pt interface where both Au and Pt have their equilibrium bulk volumes, $a_{\text{Au}} = 4.078 \text{ \AA}$ and $a_{\text{Pt}} = 3.923 \text{ \AA}$. A (111) oriented 5×5 unit cell of Au matches to a (111) oriented $3\sqrt{3} \times 3\sqrt{3}$ unit cell of Pt to better than 0.02%. For this fully relaxed Au|Pt geometry, we repeat our calculations at 300 K and obtain $\delta = 0.81 \pm 0.05$ compared to $\delta = 0.62 \pm 0.03$ with commensurable Au. This calculation indicates that the $\mathbf{k}_{\parallel} \rightarrow \mathbf{k}'_{\parallel}$ scattering does indeed lead to an increase of the interface SML. Our finding is in agreement with calculations for a Cu|Pd interface using Schep’s ansatz^{10,56} which indicated that δ increases on going from a sharp to a rough interface.¹⁴

Au|Pd.—To examine the effect of changing the strength of the SOC, we apply the procedures described above to a commensurable Au|Pd interface, choosing $a'_{\text{Au}} = a_{\text{Pd}} = 3.891 \text{ \AA}$. Corresponding to the experimental resistivity of Pd at 300 K, $\rho_{\text{Pd}} = 10.8 \mu\Omega\text{cm}$,⁴⁷ we find $l_{\text{Pd}} = 7.06 \pm 0.02 \text{ nm}$ and a value of $AR_{\text{Au|Pd}} = 0.81 \pm 0.05 \text{ f}\Omega\text{m}^2$ which is much larger than the value $0.54 \pm 0.03 \text{ f}\Omega\text{m}^2$ found for Au|Pt (inset Fig. 1, bottom panel). By substituting all the input parameters and their uncertainties into (2), we extract a value of $\delta_{\text{Au|Pd}} = 0.43 \pm 0.02$ (Fig. 1, inset). Compared to Au|Pd,

the larger SOC in Pt leads to a larger value of δ for Au|Pt. Our results for AR_I and δ for Au|Pd interfaces are in good agreement with theoretical estimates made by Belashchenko *et al.* combining Schep’s ansatz¹⁰ with calculations for ballistic Cu|Pd interfaces.¹⁴ Cu and Au have very similar electronic structures and the very different SOC of the filled 3d and 5d states below the Fermi level is not expected to play a major role.

FM|Pt interfaces.—We developed an analogous procedure to study FM|NM interfaces. Compared to the NM|NM’ case, two additional parameters enter: spin asymmetry parameters $\beta = (\rho_{\downarrow} - \rho_{\uparrow})/(\rho_{\downarrow} + \rho_{\uparrow})$ for the bulk FM and $\gamma = (R_{\downarrow} - R_{\uparrow})/(R_{\downarrow} + R_{\uparrow})$ for the interface. To avoid interfaces between a lead and Py or Co, we considered symmetric NM|FM|NM scattering geometries and studied them by passing an unpolarized charge current through them. The appropriate boundary conditions are that both the spin accumulation and spin current vanish at $z = \pm\infty$ and the analysis results in two implicit equations containing the discontinuity in the spin current at the FM|NM interface as described by $j_{s,\text{FM}}(z_I)$ and $j_{s,\text{Pt}}(z_I)$ as well as the eight transport parameters $\rho_{\text{NM}}, l_{\text{sf}}^{\text{NM}}, \rho_{\text{FM}}, l_{\text{sf}}^{\text{FM}}, \beta_{\text{FM}}, R_I, \delta$ and γ . Fig. 3(a) illustrates the spin current $j_s(z)$ that we calculate for a Pt|Py|Pt trilayer at 300 K. The five bulk parameters are determined independently as well as AR_I obtained from the Landauer formula leaving us with two equations and two unknowns, δ and γ , to be determined.

This procedure was applied to Py|Pt and Co|Pt interfaces assuming completely relaxed geometries and 8×8 interface unit cells of (111) Py or Co matched to $2\sqrt{13} \times 2\sqrt{13}$ interface unit cells of Pt. Thermal lattice and spin disorder were taken into account as described in Refs. 8, 38–40. ρ_{Pt} and l_{Pt} were already determined above and the appropriate corresponding calculations were performed for bulk Py and Co.^{40,57}

The temperature dependence of the three interface parameters that we extract for Py|Pt and Co|Pt interfaces is summarized in Fig. 3(b-d). AR_I and γ are seen to decrease monotonically with temperature for both interfaces. γ is found to vary in a small range between ± 0.15 for Py|Pt and between ± 0.03 for Co|Pt. δ , the main focus of our interest, decreases monotonically and substantially with temperature for both interfaces. $\delta_{\text{Co|Pt}}$ is larger than $\delta_{\text{Py|Pt}}$ for all temperatures in the range 200–500 K. This temperature dependence contrasts starkly with the temperature independence we found for Au|Pt. We speculate that it is the variation of the spin disorder associated with the FM magnetization that affects the interface parameters most. Consistent with this is our finding that δ and AR_I are larger for Co|Pt than for Py|Pt. With a higher Curie temperature Co is more ordered at any given temperature than Py.

To test this hypothesis, we repeated the $T = 200, 300$ and 400 K calculations for Py|Pt keeping the atomic spins ordered and including only lattice disorder in Py. The results for the three interface parameters with only lattice disorder are included in Fig. 3 (open circles, dotted lines)

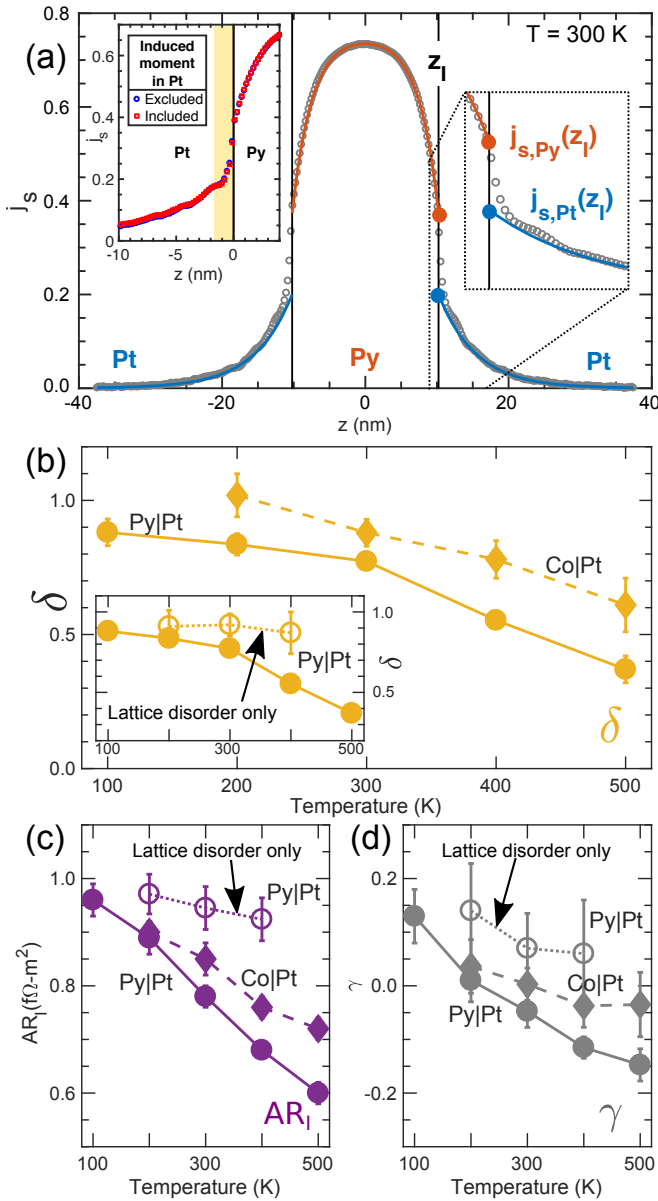


FIG. 3. (a) Open circles: spin current $j_s(z)$ through a Pt|Py|Pt trilayer calculated for $T = 300$ K. The solid blue (orange) curve is a fit to the VF equations in bulk Pt (Py). These fits are extrapolated to the interface z_I to obtain the values $j_{s,Pt}(z_I)$ and $j_{s,Py}(z_I)$ shown in detail in the right inset. The left inset shows the spin current with (red) and without (blue) proximity induced moments in Pt. (b) δ for Py|Pt (circles, solid lines) and Co|Pt (diamonds, dashed lines) plotted as a function of temperature. (Inset) δ for Py|Pt compared with results with only lattice disorder in Py|Pt (open circles, dotted lines). (c) and (d) Interface parameters AR_I and γ for Py|Pt (circles, solid and dotted lines) and Co|Pt (diamonds, dashed lines) plotted as a function of temperature. The dotted lines show the results for Py|Pt with only lattice disorder.

for comparison. With only lattice disorder included, we find that the Py|Pt interface parameters decrease much more slowly with temperature. This weak variation can

be attributed to the lattice disorder, but the decrease is much smaller compared to that brought about by spin disorder. In the low-temperature limit, we also expect δ to be smaller for Py|Pt because this interface is less abrupt than Co|Pt owing to Py's intrinsic disorder. SOC-induced interface splittings are smeared out by alloy disorder in Py compared to Co, leading to smaller δ . Lastly, we found that proximity induced magnetization of Pt by Co or Py has no effect on the interface parameters within the error bars of the calculations; see the left inset to Fig. 3(a).

Summary.— First-principles scattering theory and a recently developed local current scheme have been used to study how spin currents propagate through interfaces between two nonmagnetic (Au|Pt and Au|Pd) materials and between a ferromagnetic and a nonmagnetic (Py|Pt and Co|Pt) material at finite temperatures. By extracting values of δ , R_I and γ we could study how δ depends on various properties of the interfaces and temperature. For nonmagnetic interfaces, we found that δ and AR_I remain unchanged over a wide range of temperature and found values of AR_I that are in remarkably good agreement⁵⁶ with an *ansatz* introduced more than twenty years ago by Schep *et al.*¹⁰

$\delta_{Au|Pt}$ was found to be larger than $\delta_{Au|Pd}$ owing to the larger SOC in Pt, indicating a direct link between the magnitude of δ and SOC strength of NM metals. An incommensurate Au|Pt interface with relaxed Au and Pt lattices has a substantially larger δ than the lattice matched interface. Mixing at an interface also leads to larger values of δ . Thus to minimize δ , lattice matched and clean interfaces should be targeted in experiments to avoid momentum-nonconserving scattering of conduction electrons.

FM|Pt interface parameters decrease strongly with increasing temperature. This dependence stems directly from the magnetization of the FM. Co is a stronger FM than Py and we find that $AR_{Co|Pt}$ and $\delta_{Co|Pt}$ are larger than $AR_{Py|Pt}$ and $\delta_{Py|Pt}$ for all temperatures. By turning off spin disorder in Py|Pt, the variation of interface parameters with temperature becomes negligible.

Acknowledgements.— This work was financially supported by the “Nederlandse Organisatie voor Wetenschappelijk Onderzoek” (NWO) through the research programme of the former “Stichting voor Fundamenteel Onderzoek der Materie,” (NWO-I, formerly FOM) and through the use of supercomputer facilities of NWO “Exacte Wetenschappen” (Physical Sciences). K.G. acknowledges funding from the Shell-NWO/FOM Computational Sciences for Energy Research PhD program (CSER-PhD; nr. i32; project number 13CSER059) and is grateful to Yi Liu for help in starting this work and to S. Wildeman for helpful discussions. The work was also supported by the Royal Netherlands Academy of Arts and Sciences (KNAW). Work in Beijing was supported by the National Natural Science Foundation of China (Grant No. 61774018), the Recruitment Program of Global Youth Experts, and the Fundamental Research Funds for the

- * Email: zyuan@bnu.edu.cn
- † Email: P.J.Kelly@utwente.nl
- ¹ M. N. Baibich, J. M. Broto, A. Fert, F. Nguyen Van Dau, F. Petroff, P. Etienne, G. Creuzet, A. Friederich, and J. Chazelas, “Giant Magnetoresistance of (001)Fe/(001)Cr Magnetic Superlattices,” *Phys. Rev. Lett.* **61**, 2472–2475 (1988).
 - ² G. Binasch, P. Grünberg, F. Saurenbach, and W. Zinn, “Enhanced magnetoresistance in layered magnetic structures with antiferromagnetic interlayer exchange,” *Phys. Rev. B* **39**, 4828–4830 (1989).
 - ³ P. C. van Son, H. van Kempen, and P. Wyder, “Boundary Resistance of the Ferromagnetic-Nonferromagnetic Metal Interface,” *Phys. Rev. Lett.* **58**, 2271–2273 (1987).
 - ⁴ T. Valet and A. Fert, “Theory of the perpendicular magnetoresistance in magnetic multilayers,” *Phys. Rev. B* **48**, 7099–7113 (1993).
 - ⁵ J. Bass, “CPP magnetoresistance of magnetic multilayers: A critical review,” *J. Magn. Magn. Mater.* **408**, 244–320 (2016).
 - ⁶ J. Bass and W. P. Pratt Jr., “Spin-diffusion lengths in metals and alloys, and spin-flipping at metal/metal interfaces: an experimentalist’s critical review,” *J. Phys.: Condens. Matter* **19**, 183201 (2007).
 - ⁷ Jairo Sinova, Sergio O. Valenzuela, J. Wunderlich, C. H. Back, and T. Jungwirth, “Spin Hall effects,” *Rev. Mod. Phys.* **87**, 1213–1259 (2015).
 - ⁸ Rien J. H. Wesselink, K. Gupta, Z. Yuan, and Paul J. Kelly, “Calculating spin transport properties from first principles: spin currents,” *Phys. Rev. B* **99**, 144409 (2019).
 - ⁹ C. Galinon, K. Tewelde, R. Loloee, W.-C. Chiang, S. Olson, H. Kurt, W. P. Pratt Jr., J. Bass, P. X. Xu, K. Xia, and M. Talanana, “Pd/Ag and Pd/Au interface specific resistances and interfacial spin flipping,” *Appl. Phys. Lett.* **86**, 182502 (2005).
 - ¹⁰ Kees M. Schep, Jeroen B. A. N. van Hoof, Paul J. Kelly, Gerrit E. W. Bauer, and John E. Inglesfield, “Interface resistances of magnetic multilayers,” *Phys. Rev. B* **56**, 10805–10808 (1997).
 - ¹¹ M. D. Stiles and D. R. Penn, “Calculation of spin-dependent interface resistance,” *Phys. Rev. B* **61**, 3200–3202 (2000).
 - ¹² K. Xia, P. J. Kelly, G. E. W. Bauer, I. Turek, J. Kudrnovský, and V. Drchal, “Interface resistance of disordered magnetic multilayers,” *Phys. Rev. B* **63**, 064407 (2001).
 - ¹³ P. X. Xu, K. Xia, M. Zwierzycki, M. Talanana, and P. J. Kelly, “Orientation-Dependent Transparency of Metallic Interfaces,” *Phys. Rev. Lett.* **96**, 176602 (2006).
 - ¹⁴ K. D. Belashchenko, Alexey A. Kovalev, and M. van Schilf-gaarde, “Theory of Spin Loss at Metallic Interfaces,” *Phys. Rev. Lett.* **117**, 207204 (2016).
 - ¹⁵ Kapildeb Dolui and Branislav K. Nikolić, “Spin-memory loss due to spin-orbit coupling at ferromagnet/heavy-metal interfaces: Ab initio spin-density matrix approach,” *Phys. Rev. B* **96**, 220403(R) (2017).
 - ¹⁶ Axel Hoffmann, “Spin Hall effects in metals,” *IEEE Trans. Magn.* **49**, 5172–5193 (2013).
 - ¹⁷ M. I. Dyakonov and V. I. Perel, “Current-induced spin orientation of electrons in semiconductors,” *Phys. Lett. A* **35**, 459–460 (1971).
 - ¹⁸ J. E. Hirsch, “Spin Hall Effect,” *Phys. Rev. Lett.* **83**, 1834 (1999).
 - ¹⁹ Shufeng Zhang, “Spin Hall Effect in the Presence of Spin Diffusion,” *Phys. Rev. Lett.* **85**, 393–396 (2000).
 - ²⁰ J.-C. Rojas-Sánchez, N. Reyren, P. Laczkowski, W. Savero, J.-P. Attané, C. Deranlot, M. Jamet, J.-M. George, L. Vila, and H. Jaffrès, “Spin Pumping and Inverse Spin Hall Effect in Platinum: The Essential Role of Spin-Memory Loss at Metallic Interfaces,” *Phys. Rev. Lett.* **112**, 106602 (2014).
 - ²¹ E. Saitoh, M. Ueda, H. Miyajima, and G. Tatara, “Conversion of spin current into charge current at room temperature: Inverse spin-Hall effect,” *Appl. Phys. Lett.* **88**, 182509 (2006).
 - ²² K. Ando, S. Takahashi, K. Harii, K. Sasage, J. Ieda, S. Maekawa, and E. Saitoh, “Electric Manipulation of Spin Relaxation Using the Spin Hall Effect,” *Phys. Rev. Lett.* **101**, 036601 (2008).
 - ²³ O. Mosendz, J. E. Pearson, F. Y. Fradin, G. E. W. Bauer, S. D. Bader, and A. Hoffmann, “Quantifying spin Hall angles from spin pumping: Experiments and theory,” *Phys. Rev. Lett.* **104**, 046601 (2010).
 - ²⁴ O. Mosendz, V. Vlaminck, J. E. Pearson, F. Y. Fradin, G. E. W. Bauer, S. D. Bader, and A. Hoffmann, “Detection and quantification of inverse spin Hall effect from spin pumping in permalloy/normal metal bilayers,” *Phys. Rev. B* **82**, 214403 (2010).
 - ²⁵ Luqiao Liu, Takahiro Moriyama, D. C. Ralph, and R. A. Buhrman, “Spin-Torque Ferromagnetic Resonance Induced by the Spin Hall Effect,” *Phys. Rev. Lett.* **106**, 036601 (2011).
 - ²⁶ T. Kimura, Y. Otani, T. Sato, S. Takahashi, and S. Maekawa, “Room-Temperature Reversible Spin Hall Effect,” *Phys. Rev. Lett.* **98**, 156601 (2007).
 - ²⁷ Laurent Vila, Takashi Kimura, and YoshiChika Otani, “Evolution of the Spin Hall Effect in Pt Nanowires: Size and Temperature Effects,” *Phys. Rev. Lett.* **99**, 226604 (2007).
 - ²⁸ Yi Liu, Zhe Yuan, Rien J. H. Wesselink, Anton A. Starikov, and Paul J. Kelly, “Interface Enhancement of Gilbert Damping from First Principles,” *Phys. Rev. Lett.* **113**, 207202 (2014).
 - ²⁹ Minh-Hai Nguyen, D. C. Ralph, and R. A. Buhrman, “Spin Torque Study of the Spin Hall Conductivity and Spin Diffusion Length in Platinum Thin Films with Varying Resistivity,” *Phys. Rev. Lett.* **116**, 126601 (2016).
 - ³⁰ Edurne Sagasta, Yasutomo Omori, Miren Isasa, Martin Gradhand, Luis E. Hueso, Yasuhiro Niimi, YoshiChika Otani, and Fèlix Casanova, “Tuning the spin Hall effect of Pt from the moderately dirty to the superclean regime,” *Phys. Rev. B* **94**, 060412(R) (2016).
 - ³¹ Lei Wang, R. J. H. Wesselink, Yi Liu, Zhe Yuan, Ke Xia, and Paul J. Kelly, “Giant Room Temperature Interface Spin Hall and Inverse Spin Hall Effects,” *Phys. Rev. Lett.* **116**, 196602 (2016).
 - ³² V. P. Amin and M. D. Stiles, “Spin transport at interfaces

- with spin-orbit coupling: Formalism,” *Phys. Rev. B* **94**, 104419 (2016).
- ³³ L. J. Zhu, D. C. Ralph, and R. A. Buhrman, “Irrelevance of magnetic proximity effect to spin-orbit torques in heavy-metal/ferromagnet bilayers,” *Phys. Rev. B* **98**, 134406 (2018).
- ³⁴ Lijun Zhu, D. C. Ralph, and R. A. Buhrman, “Spin-Orbit Torques in Heavy-Metal/Ferromagnet Bilayers with Varying Strengths of Interfacial Spin-Orbit Coupling,” *Phys. Rev. Lett.* **122**, 077201 (2019).
- ³⁵ Andrew J. Berger, Eric R. J. Edwards, Hans T. Nembach, Olof Karis, Mathias Weiler, and T. J. Silva, “Determination of the spin Hall effect and the spin diffusion length of Pt from self-consistent fitting of damping enhancement and inverse spin-orbit torque measurements,” *Phys. Rev. B* **98**, 024402 (2018).
- ³⁶ Lijun Zhu, D. C. Ralph, and R. A. Buhrman, “Enhancement of spin transparency by interfacial alloying,” *Phys. Rev. B* **99**, 180404(R) (2019).
- ³⁷ Lijun Zhu, D. C. Ralph, and R. A. Buhrman, “Effective Spin-Mixing Conductance of Heavy-Metal/Ferromagnet Interfaces,” *Phys. Rev. Lett.* **123**, 057203 (2019).
- ³⁸ A. A. Starikov, Y. Liu, Z. Yuan, and P. J. Kelly, “Calculating the transport properties of magnetic materials from first-principles including thermal and alloy disorder, non-collinearity and spin-orbit coupling,” *Phys. Rev. B* **97**, 214415 (2018).
- ³⁹ Yi Liu, Anton A. Starikov, Zhe Yuan, and Paul J. Kelly, “First-principles calculations of magnetization relaxation in pure Fe, Co, and Ni with frozen thermal lattice disorder,” *Phys. Rev. B* **84**, 014412 (2011).
- ⁴⁰ Y. Liu, Z. Yuan, R. J. H. Wesselink, A. A. Starikov, M. van Schilfhaarde, and P. J. Kelly, “Direct method for calculating temperature-dependent transport properties,” *Phys. Rev. B* **91**, 220405(R) (2015).
- ⁴¹ The results we will describe are valid in the linear response regime that should be accessible using nonlocal spin-injection experiments. When properties are determined in switching experiments i.e., from spin pumping and ISHE measurements or from SHE and SOT measurements care must be taken to ensure that nonlinear effects can be neglected^{42,43}.
- ⁴² V. E. Demidov, S. Urazhdin, B. Divinskiy, V.D. Bessonov, A. B. Rinkevich, V. V. Ustinov, and S.O. Demokritov, “Chemical potential of quasi-equilibrium magnon gas driven by pure spin current,” *Nat. Commun.* **8**, 1579 (2017).
- ⁴³ I. V. Borisenko, V. E. Demidov, S. Urazhdin, A. B. Rinkevich, and S. O. Demokritov, “Relation between unidirectional spin hall magnetoresistance and spin current-driven magnon generation,” *Appl. Phys. Lett.* **113**, 062403 (2018).
- ⁴⁴ Weifeng Zhang, Wei Han, Xin Jiang, See-Hun Yang, and Stuart S. P. Parkin, “Role of transparency of platinum-ferromagnet interfaces in determining the intrinsic magnitude of the spin Hall effect,” *Nat. Phys.* **11**, 496–502 (2015).
- ⁴⁵ David V. Baxter, S. D. Steenwyk, J. Bass, and W. P. Pratt, Jr., “Resistance and spin-direction memory loss at Nb/Cu interfaces,” *J. Appl. Phys.* **85**, 4545–4547 (1999).
- ⁴⁶ K. Eid, D. Portner, J. A. Borchers, R. Loloee, M. A. Darwish, M. Tsoi, R. D. Slater, K. V. O’Donovan, H. Kurt, W. P. Pratt, Jr., and J. Bass, “Absence of mean-free-path effects in the current-perpendicular-to-plane magnetoresistance of magnetic multilayers,” *Phys. Rev. B* **65**, 054424 (2002).
- ⁴⁷ David R. Lide, ed., *CRC Handbook of Chemistry and Physics*, 90th Ed. 90th ed. (CRC Press/Taylor and Francis, Boca Raton, FL, 2009).
- ⁴⁸ The spin current flowing in the z direction and polarized along the global quantization axis of the system is defined in terms of the nonconserved spin as $j_s(z) \equiv \hat{z} \cdot \langle \sigma \otimes \mathbf{v} + \mathbf{v} \otimes \sigma \rangle / 2$. It is normalized w.r.t. the charge current density and is averaged over the xy plane perpendicular to the transport direction. For more details, see Ref. [8].
- ⁴⁹ M. Isasa, E. Villamor, L. E. Hueso, M. Gradhand, and F. Casanova, “Temperature dependence of spin diffusion length and spin Hall angle in Au and Pt,” *Phys. Rev. B* **91**, 024402 (2015).
- ⁵⁰ Ryan Freeman, Andrei Zholid, Zhiling Dun, Haidong Zhou, and Sergei Urazhdin, “Evidence for Dyakonov-Perel-like Spin Relaxation in Pt,” *Phys. Rev. Lett.* **120**, 067204 (2018).
- ⁵¹ Compared to e.g. Cu|Pt, a distinct advantage of the Au|Pt interface is that interface mixing can be studied without having to make unreasonable assumptions about the structure of the alloy. There is considerable interest in the spin-transport properties of the bulk AuPt^{52,53} (AuW⁵⁴ and AuTa⁵⁵) alloys but to do justice to this topic requires a publication in its own right; the present manuscript focusses on interfaces.
- ⁵² M. Obstbaum, M. Decker, A. K. Greitner, M. Haertinger, T. N. G. Meier, M. Kronseder, K. Chadova, S. Wimmer, D. Ködderitzsch, H. Ebert, and C. H. Back, “Tuning Spin Hall Angles by Alloying,” *Phys. Rev. Lett.* **117**, 167204 (2016).
- ⁵³ Yanjun Xu, Yumeng Yang, Hang Xie, and Yihong Wu, “Spin hall magnetoresistance sensor using $\text{au}_x\text{pt}_{1-x}$ as the spin-orbit torque biasing layer,” *Appl. Phys. Lett.* **115**, 182406 (2019).
- ⁵⁴ P. Laczkowski, J.-C. Rojas-Sánchez, W. Savero-Torres, H. Jaffrès, N. Reyren, C. Deranlot, L. Notin, C. Beigné, A. Marty, J.-P. Attané, L. Vila, J.-M. George, and A. Fert, “Experimental evidences of a large extrinsic spin Hall effect in AuW alloy,” *Appl. Phys. Lett.* **104**, 142403 (2014).
- ⁵⁵ P. Laczkowski, Y. Fu, H. Yang, J.-C. Rojas-Sánchez, P. Noel, V. T. Pham, G. Zahnd, C. Deranlot, S. Collin, C. Bouard, P. Warin, V. Maurel, M. Chshiev, A. Marty, J.-P. Attané, A. Fert, H. Jaffrès, L. Vila, and J.-M. George, “Large enhancement of the spin Hall effect in Au by side-jump scattering on Ta impurities,” *Phys. Rev. B* **96**, 140405(R) (2017).
- ⁵⁶ Schep *et al.* expressed the interface resistance in terms of the transmission through an ideal, $T=0$ K interface combined with an *ansatz* for diffusive scattering in the bulk¹⁰ inspired by random matrix theory. The predictions of this *ansatz* compare well with experiment as long as the mean free path is shorter than the distance between successive interfaces. Calculating the interface transmission without thermal disorder, with and without SOC and using Schep’s expression for the interface resistance, we find $R_{\text{Au|Pt}} = 0.63 \text{ f}\Omega\text{m}^2$ with SOC and $0.56 \text{ f}\Omega\text{m}^2$ without, compared to the room temperature value of $0.54 \pm 0.03 \text{ f}\Omega\text{m}^2$ that was found above with SOC with the present methodology.
- ⁵⁷ Kriti Gupta, *Disentangling interfaces and bulk in spin transport calculation*, Ph.D. thesis, University of Twente, The Netherlands (2019).